

Spectral Control of Cortical Activity

Sérgio Pequito [†] Arian Ashourvan ^{‡,b} Danielle Bassett ^{†,‡,b} Brian Litt ^{‡,b,‡} George J. Pappas [†]

Abstract—The proposed problem is motivated by recent studies that show that loss of consciousness is associated with the spectral evolution of the (linearized) function that models cortical activity capture by electroencephalography. In this paper, we conduct a similar study for epileptic seizure-onset where features of interest are also captured by the spectral evolution. Subsequently, one can envision a scenario where stimulating some specific brain regions (through static output feedback) one could either induce loss of consciousness, for instance, anesthesia, or prevent an epileptic seizure.

Therefore, we show that this problem consists of determining the feedback gain in the context of static output feedback for linear time-invariant switching systems that ensures the poles of the closed-loop system to remain within pre-defined closed regions. We show that this problem is NP-hard, and we explore two variants of the alternating projection method to determine its solution, to which we provide convergence guarantees not previously available in the literature.

Finally, to illustrate the main results of this paper, we conduct a brief study on epilepsy using real data and establish a potential guideline on how to tune the parameters for neurostimulators to prevent a seizure from occurring.

I. INTRODUCTION

Crafting the response of a dynamical system through feedback is in the core of the design problems in control systems engineering [1]. These dynamical systems include the electric power grid, biological systems, social networks and transportation systems, just to name a few [2].

The present paper is motivated by the recent strategies and insights in the context of cortical activity of the brain [3], [4]. More specifically, a spectral decomposition is considered for the approximation of the linearized dynamics of the cortical activity of the brain captured by electrocorticography (ECoG) electrodes. The approximation of the system's dynamics can be casted as a mode in a linear discrete-time switching system [5]; The spectral properties of the switching system can capture the nature of consciousness and cognitive states such as awake versus anesthetized states. Thus, by properly crafting the closed-loop properties one can sought to transition between the two. Similarly, they can capture the evolution of the systems during the epileptic seizure-onset [6], and, through actuation, one might be able to restrain the evolution associated with the seizure-onset.

This work was supported in part by the TerraSwarm Research Center, one of six centers supported by the STARnet phase of the Focus Center Research Program (FCRP) a Semiconductor Research Corporation program sponsored by MARCO and DARPA, and the NSF ECCS-1306128 grant.

[†]Department of Electrical and Systems Engineering, School of Engineering and Applied Science, University of Pennsylvania

[‡]Department of Bioengineering, University of Pennsylvania

^b Penn Center for Neuroengineering and Therapeutics, University of Pennsylvania

[‡] Department of Neurology, Hospital of the University of Pennsylvania

Thus, one can pose the problem of determining the static output feedback that jointly ensures spectral properties across the different modes of this system. Static output feedback entails injecting into the system a proportional (and constant over time) quantity to the collected measurements of the systems' evolution. Such strategy has the advantage of not requiring the response to a given output signal to be computed at each time instance, which might be prohibitive for large scale systems. Besides, it enables the response analysis of the closed-loop systems through its spectral decomposition. More specifically, through the analysis of the pairs of eigenvalues and eigenvectors associated with these systems. In particular, the proportional gain may enable the specification of the pairs in the spectral decomposition, hence, tuning the response of the system with respect to both system deviation from a predefined goal, modeling errors and exogenous disturbance.

Related Work: In the context deep brain stimulation and neurostimulators context, most of the strategies have considered open-loop scenarios and if-then rules [7], [8]. More recently, closed-loop strategies resorting to PID-like strategies have been also considered [9], [10]. Therefore, to the best of authors' knowledge, this is the first work presenting a control design problem as a spectral control problem, that ultimately requires to solve a problem in terms of static output feedback.

The problem of pole placement aims to determine a control law that ensures the poles of the closed-loop system to be as in a pre specified spectrum. This problem goes back to the work [11], and important landmarks where achieved in [12], where arbitrary pole placement of closed-loop by static state feedback is possible if and only if the system is controllable and observable. Nonetheless, if the pole placement is sought considering static output feedback (SOF), then the problem is NP-hard [13]. Further, in [14] it was shown that arbitrary pole placement is not achievable when SOF is considered. Notwithstanding, under certain conditions on the dimension of the state space, number of inputs and outputs, some design methods are available for relative small dimensions [15]. In addition, it has been shown that if the dimension of the state space equals the product of the number of inputs p and outputs m , then there exist $\frac{1!2!\dots(m-1)!(mp)!}{(p!(p+1)!\dots(m+p-1)!)}$ complex gain matrices that achieve any given configuration of poles of the closed-loop systems by SOF [16].

Alternatively, if the gains are only allowed to have entries within entry-wise bounds, then the SOF is still NP-hard [17]. Notwithstanding, several problems in this front still remain open [18]. Despite the complexity of these and other related problem, several efforts have been made to determine its solutions due to the significance of the problem in the context of control engineering applications [19]. In particular

in the context of stabilizing the closed-loop systems with dynamic compensators with a specified order, where several sufficient and necessary conditions using linear matrix inequalities (LMIs) are available in the literature, see for instance, [20], [21] and [22] for numerical performance evaluation. Furthermore, these results often aim to ensure the overall performance of the system in terms of a given metric, while ensuring stabilizability of either continuous- or discrete-time systems. Nonetheless, most of the numerical methods available to determine SOF gains perform poorly in practice, which motivated [23] to explore different strategies to obtain the initial conditions for iterative algorithms that determine a SOF with overall performance guarantees.

Alternatively, one might desire to ensure the poles to be within specific regions in the complex plane, hence, crafting the response behavior of the closed-loop system as presented in [24], [25], [26]. In this paper, we present a similar approach in the context of switching linear systems, where the poles of the closed-loop system in each mode are restricted to pre-specified regions in the complex plane. To the best of the authors' knowledge this is the first time that this problem is considered despite of the fact that the stabilization of switching systems in both continuous- and discrete-time has been previously addressed, see, for instance, [27], [5] and references therein. Furthermore, we present convergence guarantees that have not been previously provided in the context of static output feedback design to attain a specific pole placement. ◦

The main contributions of this paper are two-fold: (i) we leverage the cortical evolution during an epilepsy seizure-onset, and we cast the problem of mitigating a seizure as a generalized switching pole placement; and (ii) we show that the generalized switching pole placement is NP-hard, and provide two variations of the alternating projection method to determine a solution to the generalized switching pole placement, to which we present local convergence guarantees.

The rest of the paper is organized as follows. In Section II, we provide the formal problem statement. Section III reviews some concepts and terminology used in the remaining of the paper. Section IV presents the main technical results, followed by a case study in Section V showing the implications of the method in regulating the cortical activity during an epileptic seizure-onset. Conclusions and discussions on further research are presented in Section VI.

II. PROBLEM STATEMENT

The electroencephalogram (EEG) and electrocorticography (ECoG) are captured by a multivariate dynamical systems, whose local dynamical properties can be assessed using autoregressive models fitted independently to short time segments as described in [3]. This can be accomplished by considering first-order autoregressive model

$$x_{k+1} = A_k x_k + \epsilon_k, \quad k = 0, 1, \dots, \quad (1)$$

where $x_k \in \mathbb{R}^n$ is the state of the ECoG sensors at time k , and ϵ_k is an approximation error term at the same time capturing the dynamics/measurement uncertainty. This model

can be fit independently to the ECoG potentials using a least-square approach. The advantage of this approach is that it does not make any assumptions about the underlying neural mechanisms. Further, by dividing the dataset into short time segments one can estimate the evolution matrices A_k over time. Thus, not requiring the signal to remain globally stationary, and providing a good approximation of the local behavior that can be seen as stationary.

Local properties, such as stability of the system can be understood in terms of the eigenvalues of the evolution matrix A_k . These eigenvalues describe the frequency of oscillation along the corresponding eigenvector. In addition, these assess the system stability from the absolute value of the eigenvalues. Briefly, if an eigenvalue's absolute value is less than one it is asymptotic stable, and a small perturbation along the eigenvector associated with the eigenvalue will decay and return to its original trajectory. Conversely, if the absolute value of the eigenvalue is greater than one, then it is unstable, and any perturbation in the direction of the associated eigenvector will grow exponentially. Finally, those eigenvalues that are equal to one, i.e., that are the interface between asymptotic stability and instability, are referred to as *critically stable*. In practice, due to numerical precision, we classify the eigenvalues as critically stable if these are sufficiently close to the unit circumference.

In fact, it is interesting to notice that, for uneventful time windows, the eigenvalues of A_k for the corresponding period of time are concentrated in two different regions as depicted in Figure 1 (a), where a larger portion of the eigenvalues are asymptotic stable and the remaining ones are critically stable. Nonetheless, this configuration changes during either loss of consciousness (or anesthesia) and during an epileptic seizure-onset. More specifically, in the first scenario some of the critically stable eigenvalues migrate to the region containing asymptotic stability eigenvalues [4], as illustrated in Figure 1 (b). Alternatively, as we explore in Section V, during an epileptic seizure-onset some of the eigenvalues loop towards the region containing asymptotic stability eigenvalues and fully return to the critical region by the end of the seizure, as illustrated in Figure 1 (c) – see [6] for further details.

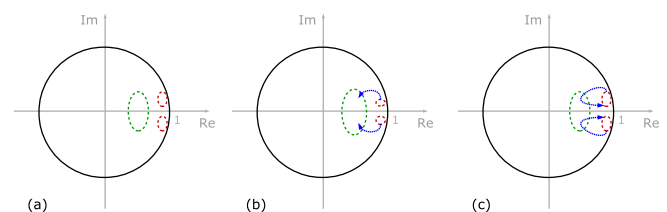


Fig. 1. In this figure, we illustrate the distribution and evolution of the eigenvalues of the linearized cortical dynamics. In green we have depicted the region where the asymptotically stable eigenvalues reside, whereas in red we identify the regions that contain the approximate critical eigenvalues. In (a) we depict the distribution of eigenvalues for the evolution matrix during uneventful periods of time. In (b), we show the evolution of a portion of eigenvalues during the period shortly after the administration of the drug for anesthesia, where the final configuration is reached during unconscious states. Finally, in (c) we depict the evolution of the eigenvalues that loop in and out of the stable regions during an epileptic seizure-onset by the blue arrow.

Now, we can consider actuation mechanisms, either invasive such as neurostimulators (or deep brain stimulation) [28], or non-invasive such as transcranial magnetic stimulation [29]. Under similar assumption, these can be captured by the following equation

$$x_{k+1} = A_k x_k + B u_k + \epsilon_k, \quad k = 0, 1, \dots, \quad (2)$$

where $u_k \in \mathbb{R}^p$ is the input injected at time k . In addition, the sensors states, i.e., the state of the system, can be also identified with the measured output of the system's cortical activity, and described as follows:

$$y_k = C x_k, \quad (3)$$

where $y_k \in \mathbb{R}^m$ correspond to the data collected at time k by the different EEG/ECOG sensors. If we assume a static output feedback controller of the form

$$u_k = K y_k, \quad (4)$$

then the closed-loop dynamics is given by

$$x_{k+1} = (A_k + BKC)x_k + \epsilon_k. \quad (5)$$

It is worth to notice that the effect of the stimulation itself on the brain tissue is non-linear, so (2) can be obtained via feedback linearization. Subsequently, assuming the validity of the local models and static output feedback, one could be interested, for instance, in the following: (i) electrically induced anesthesia, i.e., shifting the eigenvalues from a configuration in Figure 1 (a) to Figure 1 (b), or, alternatively, we can foresee a scenario where the neurostimulation steer an unconscious subject to the awake state, corresponding to shifting the eigenvalues from a configuration in Figure 1 (b) to Figure 1 (a); and (ii) restrain the evolution of the eigenvalues to the regions depicted in Figure 1 (a), i.e., forbidding the evolution depicted in Figure 1 (c), and potentially preventing a seizure from occurring.

These problems can be studied as a particular case of the *generalized switching pole placement problem* studied in the present paper formulated as follows:

\mathcal{P}_1 Given a time-varying system (2)-(3), a static output feedback described by (4), and a collection of closed subsets $\mathcal{C}_1, \dots, \mathcal{C}_n \subset \mathbb{C}$ where we want the eigenvalues of the closed-loop system to be contained, determine K such that

$$\lambda_i^k(A_k + BKC) \in \mathcal{C}_i^k, \quad i = 1, \dots, n \quad k = 0, \dots$$

where $\lambda_i^k(A_k + BKC)$ is the i -th eigenvalue of the closed-loop system described in (5). \circ

III. PRELIMINARIES AND TERMINOLOGY

In this section, we review some basic notation and terminology used in the rest of the paper.

In the sequel, for a given matrix $M \in \mathbb{C}^{r \times s}$, the vectorization operator $\text{vec}(M) \in \mathbb{C}^{rs}$ consists of the columns of M stacked below each other. We denote by $\mathbf{0}_{r \times s}$ the zero matrix in $\mathbb{C}^{r \times s}$, and, given matrices $Y \in \mathbb{C}^{m \times n}$ and $Z \in \mathbb{C}^{p \times q}$, the Kronecker product between Y and Z is denoted by the $mp \times nq$ matrix $Y \otimes Z$. Finally, we denote by $\text{Re}(Z) \in \mathbb{R}^{r \times s}$ and $\text{Im}(Z) \in \mathbb{R}^{r \times s}$ the real and imaginary parts of a matrix $Z \in \mathbb{C}^{r \times s}$.

Now, let x be an element in a Hilbert space \mathcal{H} and let \mathcal{C} be a closed (not necessarily convex) set in \mathcal{H} .

such that $\|x - c_0\| \leq \|x - c\|$ for all $c \in \mathcal{C}$ is referred to as a *projection of x onto \mathcal{C}* . In what follows, we deal with finite dimensional Hilbert spaces, where there is always at least one such point. It is known that if \mathcal{C} is a closed convex set then each point in \mathcal{H} has only one projection onto \mathcal{C} . Subsequently, we can introduce the *projection operator* onto \mathcal{C} , that is a function $\mathcal{P}_{\mathcal{C}} : \mathcal{H} \rightarrow \mathcal{H}$ such that for each $x \in \mathcal{H}$ it returns $\mathcal{P}_{\mathcal{C}}(x)$, i.e., the projection of x onto \mathcal{C} .

In this paper, we focus on a particular case of the following problem: given closed sets $\mathcal{C}_1, \dots, \mathcal{C}_N$ in a finite dimensional Hilbert space \mathcal{H} , determine a point in the intersection $\bigcap_{i=1}^N \mathcal{C}_i$ (assuming this to be non-empty). This problem is known to be solvable using the alternating projections method if all the sets are closed and convex [30]. Notice that this implicitly assumes that determining the projections in the different sets is possible. Furthermore, if the sets are non-convex, then no global convergence guarantees exist, and, in fact, it is known that for different initial conditions the alternating projections method may not converge [31].

IV. MAIN RESULTS

In this section, we present the main results of the present paper. First, we show that \mathcal{P}_1 is NP-hard (Theorem 1). Consequently, it is unlikely that an efficient algorithm to determine a solution will be available. Secondly, in \mathcal{P}'_1 , we reformulate \mathcal{P}_1 as the problem of determining K that lies in the intersection of several sets. Subsequently, we propose to solve the problem using the alternating projection algorithm. More specifically, in Algorithm 1, we propose the weighted alternating projection algorithm, whereas in Algorithm 2 we present the weighted average projection algorithm. Finally, we discuss the local convergence guarantees of both algorithms (Theorem 2).

We start by showing that solving \mathcal{P}_1 is computationally hard.

Theorem 1: The generalized switching pole placement problem described in \mathcal{P}_1 is NP-hard. \diamond

Proof: The proof follows by noticing that for the particular instance where $A_k = A$ for $k = 1, \dots, T$, i.e., when the system is linear time-invariant, and the particular case where $\mathcal{C}_i = \{c_i\}$ with $c_i \in \mathbb{C}$ for $i = 1, \dots, n$ the problem is NP-hard [13]. Hence, it follows that the problem \mathcal{P}_1 is NP-hard. \blacksquare

As a consequence of Theorem 1, it is unlikely to exist an algorithm that polynomially solves \mathcal{P}_1 . Notwithstanding, in \mathcal{P}'_1 , we propose a reformulation of \mathcal{P}_1 as the problem of determining the gain K that lies in the intersection of several sets.

Towards this goal, let \mathcal{L}_k be the set of all possible closed-loop matrices for the different evolution matrices A_k , described by

$$\mathcal{L}_k = \{L \in \mathbb{R}^{n \times n} : L = A_k + BKC \text{ for some } K\},$$

where $k = 1, \dots, T$, and T a finite-time horizon.

In addition, let \mathcal{M}_k be the set of complex matrices with eigenvalues in the specified regions $\mathcal{C}_1^k, \dots, \mathcal{C}_n^k$ given by

$$\mathcal{M}_k = \{Z \in \mathbb{C}^{n \times n} : \lambda_i(Z) \in \mathcal{C}_i^k, \quad i = 1, \dots, n\}$$

for $k = 1, \dots, T$.

As a consequence, \mathcal{P}_1 can be solved by addressing the following problem:

$$\mathcal{P}'_1 \text{ Find } X \in \mathcal{L}_1 \cap \dots \cap \mathcal{L}_T \cap \mathcal{M}_1 \cap \dots \cap \mathcal{M}_T. \quad \circ$$

Therefore, K that solves \mathcal{P}_1 (or, equivalently, \mathcal{P}'_1) can be obtained as the minimizer of $\|(C^\top \otimes B)\text{vec}(K) - \text{vec}(\text{Re}(X) - A_1)\|_2$. This follows from noticing that, in particular, K lies in the intersection of the sets \mathcal{L}_k that are convex sets, whose projection can be easily computed as follows.

Lemma 1 ([24]): The projection of $X \in \mathbb{C}^{n \times n}$ onto \mathcal{L}_k is given by $\mathcal{P}_{\mathcal{L}_k}(X) = A_k + BKC$ where $K \in \mathbb{R}^{p \times m}$ is a minimizer of $\|(C^\top \otimes B)\text{vec}(K) - \text{vec}(\text{Re}(X) - A_k)\|_2$. \circ

Nevertheless, \mathcal{M}_k is non-convex, and no easily computable projection scheme is available. Therefore, we propose to use the following approximation $\tilde{\mathcal{P}}_{\mathcal{M}_k(X)}$ instead.

Definition 1 ([24]): Let $X = VTV^*$ be the Schur's decomposition, where $V \in \mathbb{C}^{n \times n}$ is a unitary matrix and $T \in \mathbb{C}^{n \times n}$ an upper triangular matrix. The approximate projection mapping $\tilde{\mathcal{P}}_{\mathcal{M}_k}(X)$ of X onto \mathcal{M}_k is given by $\tilde{\mathcal{P}}_{\mathcal{M}_k}(X) = VT\hat{V}^*$, where

$$\hat{T}_{ij} = \begin{cases} \mathcal{P}_{\mathcal{C}_{\sigma^*(i)}^k}(T_{ii}) & \text{if } i = j, \\ T_{ij} & \text{otherwise,} \end{cases}$$

and $\sigma^* \in \Sigma$, with Σ denoting the set of possible permutations, minimizes the following optimization function

$$\sigma^* = \arg \min_{\sigma \in \Sigma} \sum_{l=1}^n |T_{ll} - \mathcal{P}_{\mathcal{C}_{\sigma(l)}^k}(T_{ll})|^2. \quad \diamond$$

The mapping in Definition 1 is motivated by the fact that if X is a symmetric matrix, then $\tilde{\mathcal{P}}_{\mathcal{M}_k}(X)$ is the best approximation of X in the Frobenius norm [24]. Further, the permutation σ^* in Definition 1 can be determined by reducing the problem to a minimum weight maximum matching. This consists in determining permutation matrices M_1 and M_2 such that they minimize the trace($M_1 \Theta M_2$), where Θ is the matrix whose entry (i, j) contains the value $|T_{ii} - \mathcal{P}_{\mathcal{C}_j^k}(T_{ii})|^2$, and $\mathcal{P}_{\mathcal{C}_j^k}(T_{ii})$ is the projection of the complex number T_{ii} onto the closed convex set \mathcal{C}_j^k . Therefore, σ^* can be described by the pairs $(i, j = \sigma^*(i))$ corresponding to the diagonal entries of $M_1 \Theta M_2$. Finally, we notice that this problem has computational complexity $\mathcal{O}(n^3)$ using, for instance, the Hungarian algorithm [32].

Next, in order to address \mathcal{P}'_1 , we propose two variations of the alternating projections method – see Algorithm 1 and Algorithm 2. The alternating projection method consists of sequentially computing the projection of a matrix in one of the sets, followed by finding the projection of the former in the another set and so forth. Nonetheless, because the projection on the sets \mathcal{M}_k is only approximated by $\tilde{\mathcal{P}}_{\mathcal{M}_k}$, in Algorithm 1, we propose to weight the ‘quality’ of the projections in the alternating projection method. This is captured by a convex combination of the projection onto a convex set and the one onto a non-convex set. More specifically, we tend to bias the approximation towards the projection onto the convex sets, whose projection can be exactly determined in a computationally efficient manner. Notice that, in theory, this does not enforce a solution to be found, but in practice it leads to a less oscillatory behavior

in the convergence to a solution. Further, if a solution has a strong bias towards the projection onto the convex sets, then it may occur that the convergence performance is degraded. Similarly, in Algorithm 2, we propose to consider a variation of the alternating projection method where one first projects onto the convex and non-convex sets, then one takes the average of these projections, and computes a weighted estimate as a starting point for the next iteration.

ALGORITHM 1: Weighted Alternating Projection Method

Input: $A_k \in \mathbb{R}^{n \times n}$, $B \in \mathbb{R}^{n \times p}$, $C \in \mathbb{R}^{m \times n}$, $\mathcal{C}_1^k, \dots, \mathcal{C}_n^k \subset \mathbb{C}$ for $k = 1, \dots, T$, and a weight $w \in (0, 1)$.

Output: The gain matrix $K^* \in \mathbb{R}^{p \times m}$ that solves \mathcal{P}_1 .

Let $Y \sim \mathcal{N}(0, \mathbb{I}_n)$, i.e., drawn from a normal distribution with zero mean and covariance matrix given by the $n \times n$ identity matrix \mathbb{I}_n . In addition, let $\epsilon > 0$ be the precision error required for the algorithm to stop.

```

1: while  $\sum_{i=1}^T \|Y - \mathcal{P}_{\mathcal{L}_i}(Y)\| + \|Y - \mathcal{P}_{\mathcal{M}_i}(Y)\| \geq \epsilon$  do
2:   for  $j = 1, \dots, T$ 
3:      $Y = w \mathcal{P}_{\mathcal{L}_j}(Y) + (1 - w) \tilde{\mathcal{P}}_{\mathcal{M}_j}(Y)$ ;
4:   end for
5: end while
```

$$K^* = \arg \min_{K \in \mathbb{R}^{p \times m}} \|(C^\top \otimes B)\text{vec}(K) - \text{vec}(\text{Re}(Y) - A_1)\|_2$$

ALGORITHM 2: Weighted Average Alternating Projection Method

Input: $A_k \in \mathbb{R}^{n \times n}$, $B \in \mathbb{R}^{n \times p}$, $C \in \mathbb{R}^{m \times n}$, $\mathcal{C}_1^k, \dots, \mathcal{C}_n^k \subset \mathbb{C}$ for $k = 1, \dots, T$, and a weight $w \in (0, 1)$.

Output: The gain matrix $K^* \in \mathbb{R}^{p \times m}$ that solves \mathcal{P}_1 .

Let $Y \sim \mathcal{N}(0, \mathbb{I}_n)$, i.e., drawn from a normal distribution with zero mean and covariance matrix given by the $n \times n$ identity matrix \mathbb{I}_n . In addition, let $\epsilon > 0$ be the precision error required for the algorithm to stop.

```

1: while  $\sum_{i=1}^T \|Y - \mathcal{P}_{\mathcal{L}_i}(Y)\| + \|Y - \mathcal{P}_{\mathcal{M}_i}(Y)\| \geq \epsilon$  do
2:    $PL_{\text{aux}} = \mathbf{0}_{n \times n}$ ;
3:    $PM_{\text{aux}} = \mathbf{0}_{n \times n}$ ;
4:   for  $j = 1, \dots, T$ 
5:      $PL_{\text{aux}} = PL_{\text{aux}} + \mathcal{P}_{\mathcal{L}_j}(Y)$ ;
6:      $PM_{\text{aux}} = PM_{\text{aux}} + \mathcal{P}_{\mathcal{M}_j}(Y)$ ;
7:   end for
8:    $Y = w \frac{PL_{\text{aux}}}{T} + (1 - w) \frac{PM_{\text{aux}}}{T}$ ;
9: end while
```

$$K^* = \arg \min_{K \in \mathbb{R}^{p \times m}} \|(C^\top \otimes B)\text{vec}(K) - \text{vec}(\text{Re}(Y) - A_1)\|_2$$

Notice that the overall complexity of the algorithm consists in sequentially solving convex optimization problem (e.g., using CVX), and computing the projection on the sets \mathcal{M}_k which requires the computation of an eigenvalue-eigenvector decomposition and an assignment problem. Henceforth, leading to computationally tractable optimization problem; specifically, the number of variables considered in the context of the problem motivated in this paper is usually small, and consists in the number of electrodes placed in the surface of the cortex.

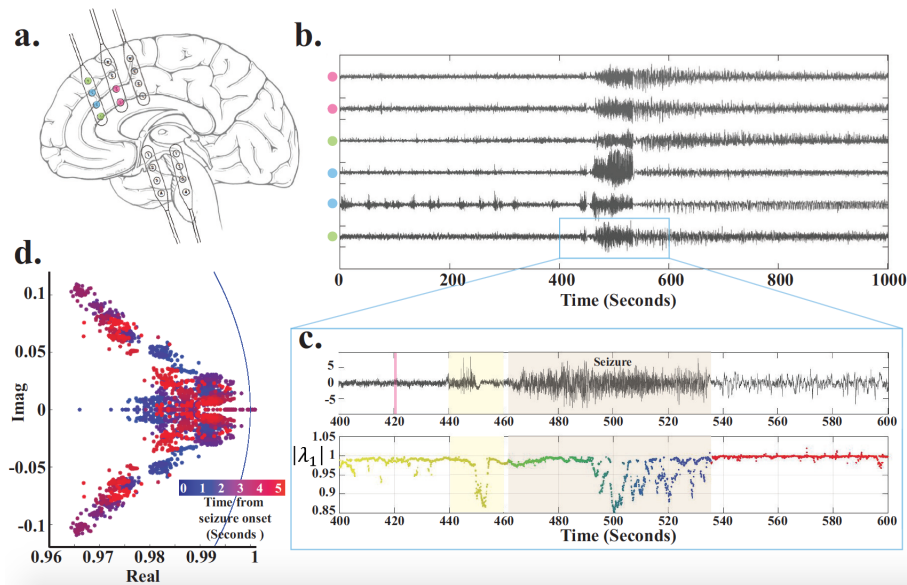


Fig. 2. In (a) we depict the location of the ECoG electrode placed over the right medial structures. The 6 color-coded electrodes were selected for further analysis. The pink circles indicate the location of the measuring electrodes, whereas the cyan circles indicate that both measuring and actuation capabilities are available. In (b), we provide the normalized (z-score) times-courses of these 6 electrodes over a 1000s window around a seizure-event. In addition, in the top figure in (c) we zoom-in the evolution from 400 to 600, whereas in the bottom figure we represents the absolute value of the ‘largest’ eigenvalue of the approximate dynamics prior to (yellow dots), during (green-blue dots), and after (red dots) the seizure event. The duration of the sliding-window to estimate the model, the pre-seizure period, and the seizure event are highlighted with transparent, pink, yellow, and brown regions, respectively. Finally, in (d) the temporal evolution of the eigenvalues is color-coded to highlight early excursion of some eigenvalues from the critical regime to asymptotically stable regime during the seizure-onset followed by their return back to departure region. In particular, this behavior was previous illustrated in Figure 1 (c), which was on the motivation basis of the proposed solution.

Now, we discuss some local convergence properties guarantees, as well as convergence rates, that can be provided for the generalized switching pole placement, if we assume that the exact projections on the convex and non-convex sets are available. Notice that both sets \mathcal{L}_k and \mathcal{M}_k are super-regular sets, since these sets can be associated with semi-algebraic functions – those functions whose graphs are composed of finitely many sets, each defined by finitely many polynomial inequalities. Subsequently, from [33], local linear convergence guarantees are available for both Algorithm 1 and Algorithm 2 as stated next.

Theorem 2: Let Y in Algorithm 1 and Algorithm 2 be such that $\|Y - X^*\| < \varepsilon$, where X^* is a solution to \mathcal{P}'_1 (assuming it exists), for a small $\varepsilon > 0$. Then, Algorithm 1 and Algorithm 2 converge to X^* , and these have the following linear convergence rates

$$r_{\text{av}} \leq 1 - \frac{1}{2\kappa^2} \text{ and } r_{\text{alt}} \leq 1 - \frac{1}{\kappa^2},$$

respectively, where κ is the infimum that satisfies the following inequality

$$\sqrt{\sum_i \|y_i\|^2} \leq \kappa \left\| \sum_i y_i \right\|,$$

for $y_i \in N_{\mathcal{F}_i}(\bar{x})$, where \mathcal{F}_i ($i = 1, \dots, m$) are close sets and

$N_{\mathcal{F}}(\bar{x}) = \{\lim_i t_i(x_i - z_i) : t_i \geq 0, x_i \rightarrow \bar{x}, z_i \in \mathcal{P}_{\mathcal{F}}(x_i)\}$, is the normal cone to a closed set \mathcal{F} at a point $\bar{x} \in \mathcal{F}$. \diamond

Proof: First, we notice that the weighting factor considered in Algorithm 1 and Algorithm 2 consists of a positive scaling of the sets and corresponding projection value. In other words, the properties of convexity and non-convexity

of the sets remain unchanged by the positive scaling. Furthermore, even if the exact projection is not available, the alternating projection methods can conserve convergence properties as soon as the approximation error is sufficiently ‘small’, see [33] for details. Therefore, by considering the weighted alternating projection method in both Algorithm 1 and Algorithm 2, one can choose w sufficiently close to 1 such that the error resulting from $\tilde{\mathcal{P}}_{\mathcal{M}_k}$ is small enough to ensure that local convergency guarantees hold. \blacksquare

Remark that the alternating projection algorithm has better convergence performance than the average projection algorithm, yet the required condition to obtain such convergence results are different. In particular, the convergence of the average projection algorithm does not require the assumption of super-regularity, which is required for the convergence of the alternating projection algorithm.

Regardless, one should keep in mind the fact that the problem is NP-hard and global guarantees are unlikely to exist. Further, in practice, both algorithms are quite sensitive to the initialization, and several trials or strategies need to be employed to obtain feasible solutions, see [23].

V. REGULATION OF CORTICAL ACTIVITY

In this section, we explore in detail the application of the aforementioned methods in the context of epileptic seizures, i.e., the characterization and control of the seizure-onset properties. We studied the ECoG recorded data (500 Hz) during focal complex partial seizures [34] from a single neocortical epilepsy patient undergoing routine pre-surgical evaluation of her epilepsy [35]. During the recording session, the patient had four seizures lasting tens of seconds.

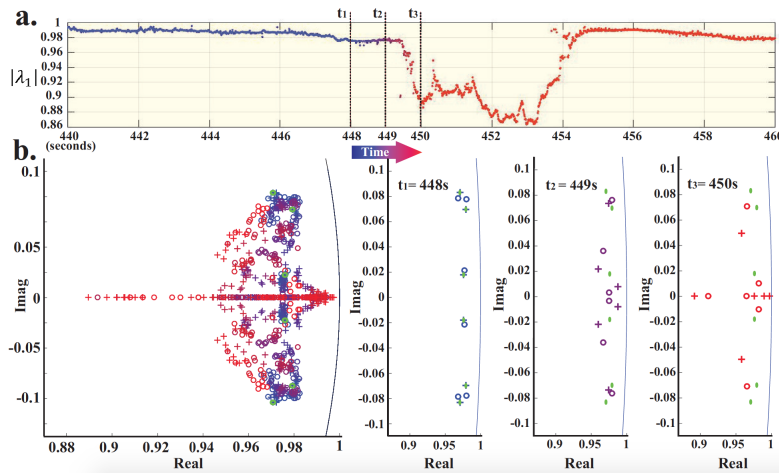


Fig. 3. In (a) we represent the zoomed in version of the pre-seizure period (yellow region) displayed in Figure 2 (c). Plot (b), in the first graph (on the left hand-side), we display the location of eigenvalues of A_k , $k = 1, \dots, 200$ (marked by '+') and the corresponding closed-loop system of $A_k + BKC$ (marked by 'o') for several time points over the stretch of 2 seconds. The increasing temporal ordering of the eigenvalues are color-coded by blue-to-red gradient. Observe that the vast majority of the closed-loop eigenvalues are placed close to the unit circle, i.e., the critical zones. These results are more discernible in right hand-side, where several snapshots of the eigenvalues of A_k and the close-loop system are provided separately ($t_1 - t_3$).

Figure 2 (b) displays the normalized (z-scored) time-courses of the recorded signal from 6 right medial anterior frontal electrodes (marked with colored circles in Figure 2 (a)) over the peri-seizure period. Prior to some of these events the patient had a feeling of wooziness. During these events, the patient was noted to display semi-purposeful and automatic behavior predominantly in the right upper extremity.

We fit the model (1) to short overlapping temporal windows (window length of 2s, with 10ms shifts) of the 6 ECoG channels' depicted in Figure 2 (a). From Figure 2 (d), there is strong evidence that the seizure-onset can be characterized by gradual departure from critical to more asymptotically stable regimes followed by periods of higher frequency during the asymptotically stable period. As seen in Figure 2 (c), the seizure ends when the eigenvalues slowly settle in a critically stable regime.

To test the robustness of our observation to the choice of parameters, we repeated the analysis for several other electrode sets (with different number and locations of electrodes) and window sizes. Overall, the aforementioned pattern of change in the stability of the eigenvalues during the seizure-onset period remained qualitatively the same regardless of the parameter choices. A detailed study on the characterization of the seizure-onset is provided in [6], which can be attained by exploiting the eigenvalue-eigenvector structure of the system's dynamics.

Interestingly in this example, the eigenvalues display a similar transition cycle to that of the seizure-onset period eigenvalues, though only lasting for few seconds, starting around 20 seconds prior to the seizure onset. We will focus on this period prior to the seizure-onset since is causally related with the seizure itself. Therefore, by crafting its evolution one is likely to mitigate the seizure itself. In particular, this is achieved by addressing the generalized switching pole placement introduced in this paper. Notwithstanding, we notice that the validation of the results needs to be taken in consideration with caution, since the closed-loop is being

performed only on the linearization of the cortical dynamics, and the nonlinear effect can be captured by considering feedback linearization; thus, reducing to the setup presented in this paper. Simply speaking, some unexpected behavior might be unveiled when applying these strategies in a clinical setting, and some additional nonlinear modeling needs to be taken in consideration.

Next, using the weighted alternating projection method (Algorithm 1), with weighting parameter of $w = 0.1$, and the A_k , $k \in \{1, \dots, 200\}$, for a 1s window within a period prior to the seizure-onset period highlighted in yellow in Figure 2 (c) and Figure 3 (a). Similar results could be attained using the weighted average alternating projection method (Algorithm 2), which we do not report due to space constraints. Furthermore, we set the desirable location to be within an ellipse centered around the eigenvalues of A_1 with the x -radius equal to 0.001 and y -radius equal to 0.0015. Notice that for such constraints a solution, i.e., a gain, that solves \mathcal{P}'_1 may not exit, so the intended goal is to keep the eigenvalues closer to the critically stable regions, i.e., closer to the distribution of the eigenvalues of a dynamics matrix during a healthy state. Therefore, regardless of the size of the final desired regions, the locations attained in this experiment are clinically relevant for the analysis of the seizure intervention. In addition, we assume that the input and output matrices are described by two canonical vectors in \mathbb{R}^6 with the nonzero entries associated with the electrodes depicted in blue and cyan in Figure 2 (a), respectively. As result, the gain matrix determined is as follows:

$$K = \begin{bmatrix} 0.0306 & -0.0674 \\ 0.0595 & -0.0382 \end{bmatrix}.$$

Figure 3 (b) shows the plot of all eigenvalues of the evolution matrix A_k (marked by '+') and its closed-loop system (marked by 'o'). As mentioned earlier, although the algorithm does not necessarily place the eigenvalues within the specified convex regions, we were able to achieve the goal of placing the eigenvalues back closer to the critical zone (see Figure 3 (b)), through the tuning of parameters

such as the size of the convex regions.

In summary, these results suggest that by actuating the system with static output feedback one can obtain a gain to successfully steering the eigenvalues of the system back to the healthy regime at any given time point prior the seizure-onset period. Thus, potentially mitigating the existence of an epileptic seizure in a later stage.

VI. CONCLUSIONS AND FURTHER RESEARCH

In this paper, we introduced a spectral characterization for the study for epileptic seizure-onset. Subsequently, we sought to develop a closed-loop actuation strategy that is cast as a static output feedback for linear time-invariant switching systems. More specifically, the goal consists in ensuring the poles of the closed-loop system to remain within pre-defined closed regions associated with a healthy regime. We showed that this problem is NP-hard, and we provided two variants of the alternating projection method to determine its solution, to which we provided local convergence guarantees. Also, we conducted a brief study on epilepsy using real data as a proof-of-concept, and establish a potential guideline on how to tune the parameters for neurostimulators to mitigate the effect of epileptic seizures.

These is one attempt to formalize the parameterization of the neurostimulators, and further validation in closed-loop settings is required. Therefore, we are currently pursuing such validation in larger datasets, such that a validation of the approach can be justified by the clinician in the context of epilepsy treatment. Furthermore, we are pursuing validation in different settings as mentioned before, i.e., anesthesia. On a different note, we are also pursuing the development of iterative algorithms with better performances guarantees and capable of dealing with additional constraints on the gain need to be studied, such that more realistic setups can be accounted for.

REFERENCES

- [1] S. Skogestad and I. Postlethwaite, *Multivariable Feedback Control: Analysis and Design*. John Wiley & Sons, 2005.
- [2] K. J. Aström and P. Kumar, "Control: A perspective," *Automatica*, vol. 50, no. 1, pp. 3–43, Jan. 2014.
- [3] G. Solovey, K. J. Miller, J. Ojemann, M. O. Magnasco, and G. A. Cecchi, "Self-regulated dynamical criticality in human ECoG," *Frontiers in Integrative Neuroscience*, vol. 6, no. 44, 2012.
- [4] G. Solovey, L. M. Alonso, T. Yanagawa, N. Fujii, M. O. Magnasco, G. A. Cecchi, and A. Proekt, "Loss of consciousness is associated with stabilization of cortical activity," *The Journal of Neuroscience*, vol. 35, no. 30, pp. 10866–10877, 2015.
- [5] H. Lin and P. J. Antsaklis, "Stability and stabilizability of switched linear systems: A survey of recent results," *IEEE Transactions on Automatic Control*, vol. 54, no. 2, pp. 308–322, Feb 2009.
- [6] A. Ashourvan, S. Pequito, S. N. Baldassano, A. Khambhati, J. M. Vettel, B. Litt, G. J. Pappas, and D. Bassett, "Multichannel intracranial eeg seizure-onset assessment via dynamical systems stabilizability," *Under Review*, 2017.
- [7] M. J. Morrell and C. Halpern, "Responsive direct brain stimulation for epilepsy," *Neurosurgery Clinics of North America*, vol. 27, no. 1, pp. 111 – 121, 2016, epilepsy.
- [8] V. Krishna, F. Sammartino, N. K. K. King, R. Q. Y. So, and R. Wennberg, "Neuromodulation for epilepsy," *Neurosurgery Clinics of North America*, vol. 27, no. 1, pp. 123 – 131, 2016, epilepsy.
- [9] J. Echauz, H. Firpi, and G. Georgoulas, "Intelligent control strategies for neurostimulation," in *Applications of intelligent control to engineering systems*. Springer, 2009, pp. 247–263.
- [10] A. O. Hebb, J. J. Zhang, M. H. Mahoor, C. Tsiokos, C. Matlack, H. J. Chizeck, and N. Pouratian, "Creating the feedback loop: Closed-loop neurostimulation," *Neurosurgery Clinics of North America*, vol. 25, no. 1, pp. 187 – 204, 2014, advances in Neuromodulation.
- [11] W. Levine and M. Athans, "On the determination of the optimal constant output feedback gains for linear multivariable systems," *IEEE Transactions on Automatic Control*, vol. 15, no. 1, pp. 44–48, Feb 1970.
- [12] W. Wonham, "On pole assignment in multi-input controllable linear systems," *IEEE Transactions on Automatic Control*, vol. 12, no. 6, pp. 660–665, December 1967.
- [13] M. Fu, "Pole placement via static output feedback is NP-hard," *IEEE Transactions on Automatic Control*, vol. 49, no. 5, pp. 855–857, May 2004.
- [14] A. Eremenko and A. Gabrielov, "Counterexamples to pole placement by static output feedback," *Linear Algebra and its Applications*, vol. 351352, pp. 211 – 218, 2002, fourth Special Issue on Linear Systems and Control.
- [15] A. Morse, W. Wolovich, and B. Anderson, "Generic pole assignment: Preliminary results," *IEEE Transactions on Automatic Control*, vol. 28, no. 4, pp. 503–506, Apr 1983.
- [16] R. Brockett and C. Byrnes, "Multivariable nyquist criteria, root loci, and pole placement: A geometric viewpoint," *IEEE Transactions on Automatic Control*, vol. 26, no. 1, pp. 271–284, Feb 1981.
- [17] V. D. Blondel and J. N. Tsitsiklis, "Survey a survey of computational complexity results in systems and control," *Automatica*, vol. 36, no. 9, pp. 1249–1274, Sep. 2000.
- [18] J. Rosenthal and J. C. Willems, *Open Problems in Mathematical Systems and Control Theory*. London: Springer London, 1999, ch. Open problems in the area of pole placement, pp. 181–191.
- [19] V. Syrmos, C. Abdallah, P. Dorato, and K. Grigoriadis, "Static output feedback a survey," *Automatica*, vol. 33, no. 2, pp. 125 – 137, 1997.
- [20] J. C. Geromel, P. Colaneri, and P. Bolzern, "Dynamic output feedback control of switched linear systems," *IEEE Transactions on Automatic Control*, vol. 53, no. 3, pp. 720–733, April 2008.
- [21] J. C. Geromel, C. C. de Souza, and R. E. Skelton, "Static output feedback controllers: stability and convexity," *IEEE Transactions on Automatic Control*, vol. 43, no. 1, pp. 120–125, Jan 1998.
- [22] M. C. de Oliveira and J. C. Geromel, "Numerical comparison of output feedback design methods," in *American Control Conference, 1997. Proceedings of the 1997*, vol. 1, Jun 1997, pp. 72–76 vol.1.
- [23] Y. J. Peretz, "A randomized approximation algorithm for the minimal-norm static-output-feedback problem," *Automatica*, vol. 63, pp. 221 – 234, Jan 2016.
- [24] K. Yang and R. Orsi, "Generalized pole placement via static output feedback: A methodology based on projections," *Automatica*, vol. 42, no. 12, pp. 2143–2150, Dec. 2006.
- [25] A. Hassibi, J. How, and S. Boyd, "A path-following method for solving bmi problems in control," in *Proceedings of the American Control Conference*, vol. 2, Jun 1999, pp. 1385–1389 vol.2.
- [26] A. Satoh, J. Okubo, and K. Sugimoto, "Transient response shaping in H-infinity; control by eigenstructure assignment to convex regions," in *Proceedings of the 42nd IEEE Conference on Decision and Control*, vol. 3, Dec 2003, pp. 2288–2293 Vol.3.
- [27] J. C. Geromel and P. Colaneri, "Stability and stabilization of discrete time switched systems," *International Journal of Control*, vol. 79, no. 7, pp. 719–728, 2006.
- [28] J. S. Perlmutter and J. W. Mink, "Deep brain stimulation," *Annual review of neuroscience*, vol. 29, pp. 229–257, 2006.
- [29] Z. J. Daskalakis, B. K. Christensen, P. B. Fitzgerald, and R. Chen, "Transcranial magnetic stimulation," *The Journal of Neuropsychiatry and Clinical Neurosciences*, vol. 14, no. 4, pp. 406–415, 2002, PMID: 12426408.
- [30] L. Gubin, B. Polyak, and E. Raik, "The method of projections for finding the common point of convex sets," *USSR Computational Mathematics and Mathematical Physics*, vol. 7, no. 6, pp. 1 – 24, 1967.
- [31] P. L. Combettes and H. J. Trussell, "Method of successive projections for finding a common point of sets in metric spaces," *Journal of Optimization Theory and Applications*, vol. 67, no. 3, pp. 487–507, 1990.
- [32] H. W. Kuhn and B. Yaw, "The hungarian method for the assignment problem," *Naval Res. Logist. Quart.*, pp. 83–97, 1955.
- [33] A. S. Lewis, D. R. Luke, and J. Malick, "Local linear convergence for alternating and averaged nonconvex projections," *Foundations of Computational Mathematics*, vol. 9, no. 4, pp. 485–513, 2009.
- [34] K. E. Misulis, "Atlas of EEG, seizure semiology, and management," Oxford, UK.
- [35] *International Epilepsy Electrophysiology Portal website*. [Online]. Available: <http://www.ieeg.org>